



# The impact of COVID-19 lockdown on surface air quality changes in major African countries

Zizhen Han<sup>1</sup>, Yuqiang Zhang<sup>1\*</sup>, Zhou Liu<sup>1</sup>, Kexin Zhang<sup>2,3</sup>, Zhuyi Wang<sup>1</sup>, Bin Luo<sup>1</sup>, Likun Xue<sup>1</sup>, Xinfeng Wang<sup>1\*</sup>

5 <sup>1</sup> Environmental Research Institute, Shandong University, Qingdao 266237, China

<sup>2</sup> School of Environmental Science and Engineering, Shandong University, Qingdao 266237, China

<sup>3</sup> Shenzhen Key Laboratory of Ecological Remediation and Carbon Sequestration, Institute of Environment and Ecology, Tsinghua Shenzhen International Graduate School, Tsinghua University, Shenzhen 518055, China

Correspondence to: Yuqiang Zhang ([yuqiang.zhang@sdu.edu.cn](mailto:yuqiang.zhang@sdu.edu.cn)), Xinfeng Wang ([xinfengwang@sdu.edu.cn](mailto:xinfengwang@sdu.edu.cn))

## 10 Abstract.

The lockdown during the coronavirus disease 2019 (COVID-19) pandemic provides a natural experience to examine the air quality changes from emission reductions. However, limited monitoring data has made it challenging to study these changes in major African regions. This study aimed to assess air quality changes, including major pollutants such as CO, NO<sub>2</sub>, O<sub>3</sub>, SO<sub>2</sub>, and aerosol particles during COVID-19 lockdowns in 2020 across different African countries. Using chemical reanalysis products from the Jet Propulsion Laboratory, we calculated quarterly dual anomalies and quarterly anomalies for MAM (March to May) and JJA (June to August) in 2020. Results showed a general decline in CO, NO<sub>2</sub>, O<sub>3</sub>, and nitrate aerosol across majority African countries, with more pronounced decreases during JJA. However, discrepancies were also seen: quarterly dual anomalies revealed a decrease in NO<sub>2</sub> and SO<sub>2</sub> in Northern Africa (NA), while quarterly anomalies showed an increase, suggesting containment policies moderated the increase rates. In Southern Africa (SA), both methods observed increases in SO<sub>2</sub>, likely due to relaxed restrictions and heightened energy demands. Sensitivity diagnostics showed that the increase in O<sub>3</sub> in South Africa may be related to the decrease in NO<sub>2</sub>. Additionally, increased sulfate and ammonium aerosols in NA and SA was likely attributed to dust events and higher residential emissions, respectively. For this study, we concluded that air quality changes may be intertwined with both natural and anthropogenic influences and the results highlight the necessity for stricter emission standards for coal-fired plants and promote clean energy in African countries.

25



## 1 Introduction

The strict containment policies during the outbreak of coronavirus disease 2019 (referred to as COVID-19) in 2020, such as partial or complete closure of international borders, schools, and non-essential businesses, as well as restrictions on citizen  
30 movement in some cases (Pepe et al., 2020), provided a natural experiment to investigate how the air quality will respond to potential strict control policies (Navinya et al., 2020; Sikarwar and Rani, 2020; Singh and Chauhan, 2020). Numerous studies have investigated the air quality changes due to the lockdown measures across different worldwide regions using surface observation, air quality modelling and satellite retrievals. However, the responses of the air quality changes were highly depending on the species and location, and were not always consistent.

35

Many studies have shown that strict lockdown measures have led to significant improvements for certain pollutants, but no noticeable decrease for the other. Take a few as example, the cities of Chongqing, Luzhou, and Chengdu in China experienced the largest decreases in NO<sub>2</sub> and sulfur dioxide (SO<sub>2</sub>) by 62.1% and 83.8% individually during February 2020 when compared with the same month in previous years (2017–2019), while carbon monoxide (CO), PM<sub>10</sub>, and PM<sub>2.5</sub> had relatively smaller  
40 decreases, ranging from 17.9% to 30.8%. Surprisingly, O<sub>3</sub> concentration increased by 6.2% instead (Zhang et al., 2020). In addition, although reduced anthropogenic emissions during the lockdown period led to an obvious decrease in PM<sub>2.5</sub> across most provinces in China, unfavourable weather conditions, mainly less rainfall, lower planetary boundary layer (PBL) and wind speed, higher relative humidity (RH) and temperature, resulted in only half of its precursor's decline (Wang et al., 2020). During the recent lockdown period in Shanghai, China from April to May 2022, both surface and column NO<sub>2</sub> were observed  
45 a significantly decreases. However, surface formaldehyde (HCHO) was found to increase by 13%, and O<sub>3</sub> had no significant changes due to the weakened titration effects from reduction in NO (Tan and Wang, 2022). As one of the cities severely affected by the COVID-19 pandemic after Wuhan, Milan in Italy also observed a significant decrease in NO<sub>2</sub> during the lockdown period. However, while there was a 20% reduction in SO<sub>2</sub> concentration in urban areas, there was no change in SO<sub>2</sub> levels in suburban areas, possibly due to more closures of public places in urban areas resulting in a decrease in heating demand,  
50 but the suburban heating demand has not dropped significantly. Meanwhile, O<sub>3</sub> concentrations significantly increased in urban areas, which could be attributed to chemical oxidation reactions caused by increased sunlight hours and decreased NO<sub>2</sub> concentrations (Collivignarelli et al., 2020). During the lockdown period, NO<sub>2</sub> concentrations were also found to decrease significantly in the United States (Goldberg et al., 2020; Muhammad et al., 2020; Qu et al., 2021), while PM<sub>2.5</sub> only decreased in metropolitan areas of Northeastern and California/Nevada regions with O<sub>3</sub> concentrations remaining relatively stable (Chen  
55 et al., 2020c). Similar phenomena has also been found in other countries such as India (Navinya et al., 2020; Mor et al., 2021), Bangladesh (Kganyago and Shikwambana, 2021), Brazil (Siciliano et al., 2020), Spain (Baldasano et al., 2020), and EU member states (Varga et al., 2024). Meanwhile a few studies also investigated the impact of lockdown measures on air quality changes from a global perspective (Venter et al., 2020; Miyazaki et al., 2021; Sekiya et al., 2023), with assimilated high-resolution OMI and TROPOMI satellite retrievals or ground observation data. It was found that although global anthropogenic



60 NO<sub>2</sub> emissions decreased significantly during the lockdown periods in 2020, the decreases in PM<sub>2.5</sub> were smaller than that of  
NO<sub>2</sub> or even remained unchanged (Venter et al., 2020; Chossière et al., 2021; Shi et al., 2021). Additionally, due to the high  
local ozone production efficiency in Asia and America, there were little changes in the global tropospheric ozone burden  
(Miyazaki et al., 2021). Furthermore, Shi et al. (2021) discovered that the decreases in NO<sub>2</sub> concentrations in 11 typical cities  
65 were lower than expected through deweathering machine learning techniques, indicating the importance of weather conditions  
on the air quality changes. However, to our best knowledge, few studies have been focused on African continent mainly due  
to the lack of well-developed ground monitoring sites and the lack of attention and funding for the African environment (Mead  
et al., 2023).

As the region with the highest exposure to PM<sub>2.5</sub> in the world, Africa's air pollution problem cannot be overlooked. With the  
70 rapid urbanization, economic development, and increasing reliance on fossil fuel combustion (Garcia et al., 2021; Katoto et  
al., 2019; Navaratnam et al., 2024), the air pollution-induced mortality burden has become the second leading cause of death  
in Africa (Health Effects Institute, 2022; Fisher et al., 2021). The epidemic lockdown has also provided an “opportunity  
scenario” to investigate the effectiveness of emission reduction policies to improve air quality in African countries. Some  
available studies have been carried out to study the air quality changes in specific African cities or regions by utilizing sporadic  
75 monitoring station data (Khomsi et al., 2021) and remote sensing (Yusuf et al., 2021). For example, in several cities of  
Morocco, during the lockdown period, there was a significant decrease in NO<sub>2</sub> compared with before the lockdown, and PM<sub>2.5</sub>  
also relatively decreased (Singh et al., 2020b; Khomsi et al., 2020, 2021). In some cities in Nigeria, O<sub>3</sub> concentration increased  
slightly, while NO<sub>2</sub> concentration decreased in March but slightly increased in April. SO<sub>2</sub> concentration during the lockdown  
months (March and April) increased compared with previous years but exhibited a lower level than January and February  
80 (Fuwape et al., 2020). Using OMI retrieved data, NO<sub>2</sub> emissions decreased by 15% and 33% in Cairo and Alexandria of Egypt  
respectively, with slight decrease of CO (approximately 5%), and increase of ozone by about 2% compared with the years  
2015-2019 (Mostafa et al., 2021). In Kampala, Uganda, one of busiest cities in Eastern Africa, the Air Quality Index (AQI)  
showed a 6.6% decrease during the lockdown period (March to July) compared with the previous year (Abisha Meji et al.,  
2020).

85

The main purpose of this study is to investigate the concentration changes of gas and aerosol pollutants during COVID-19  
lockdown periods in major African continents during the boreal spring (March to May, referred as MAM) and boreal summer  
(June to August, referred as JJA) seasons. We utilize chemical reanalysis products from the state-of-the-art multi-component  
satellite data assimilation system (Miyazaki et al., 2020a; Miyazaki et al., 2020c; Miyazaki et al., 2021), which optimizes  
90 pollutant concentrations and emissions by assimilating multiple satellite observations and considering chemical interactions  
between different gases. To isolate the effects of temporal emission changes and interannual meteorological variations, we  
applied two distinct methods in quantifying the air quality changes, including the quarterly mean anomalies (the difference in  
pollutant concentration between 2020 and reference years (2005-2019)), and difference-to-difference (the difference between



the February mean anomaly and the quarterly mean anomaly). We also calculated the Pearson correlation coefficients between  
95 pollutant concentrations changes and stringency index or meteorological condition changes to quantify and compare their  
strengths of correlation during the MAM and JJA.

## 2 Data and methodology

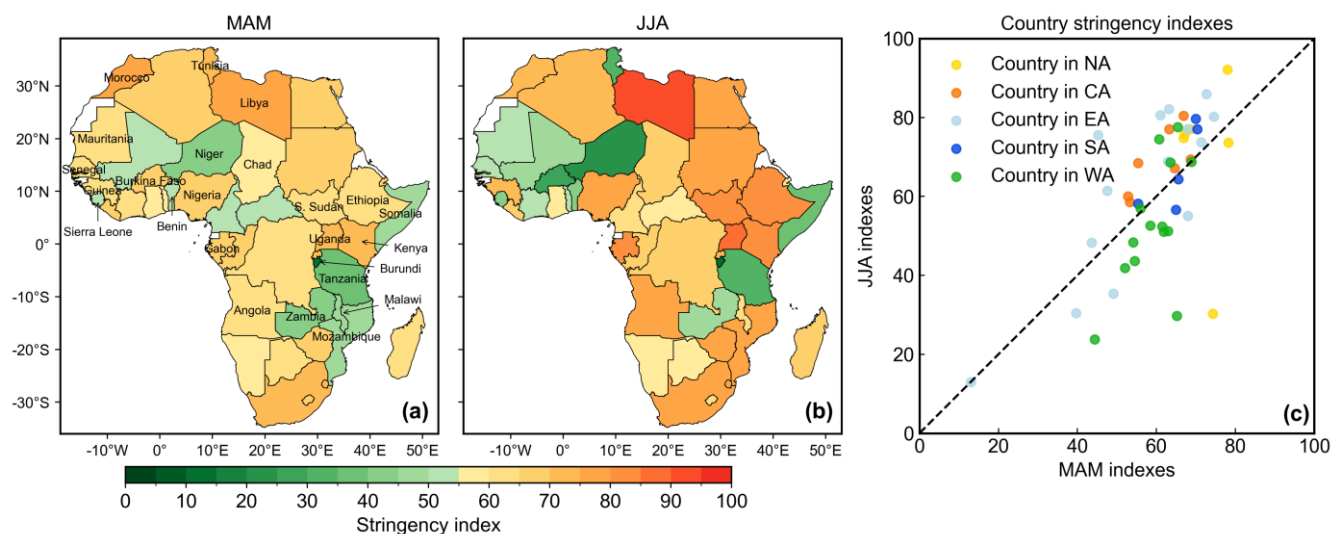
### 2.1 Study area

Figure S1 shows the map of the study area which covers the whole Africa continent including 50 countries which lies between  
100 40°S–40°N and 20°W–40°E, except some islands such as Cabo Verde, São Tomé and Príncipe, Comoros, Mauritius, Mayotte,  
Réunion, Seychelles and Saint Helena. We further separated Africa countries into the following regions, including Northern  
Africa (NA), Central Africa (CA), Western Africa (WA), Eastern Africa (EA), Southern Africa (SA) as adopted by United  
Union (Fig. S1).

### 2.2 Government restrictions in Africa

105 Since March 2020, African countries have implemented different restrictive policies in response to the COVID-19 pandemic.  
We obtained the indicator of the lockdown stringency measures developed by (Hale et al., 2021) to quantify the containment  
intensity in African countries. The index, which ranges from 0 to 100 (Fig. S2), tracks the multiple measures and responses to  
the COVID-19 crisis over time at a daily resolution, including school and workplace closings, public transport closings,  
international travel restrictions, and so on. From Figure 1 we can see that overall, the stringency index in the African continent  
110 is higher in JJA than those in MAM, meaning that the lockdown measures were generally stricter, such as Mozambique,  
Ethiopia, S. Sudan, Libya, Malawi, Guinea, Uganda and Nigeria. As shown in Figure 1c, the stringency indexes of all CA  
countries have increased in the JJA compared to the MAM, while other regions in Africa have mixed changes. There were 18  
countries where the stringency index in the MAM was higher than those in the JJA, such as Tunisia, Burkina Faso, Niger,  
Somali, Mauritania, Sierra Leone, Senegal, Benin. In MAM, the countries with the highest stringency index include Morocco  
115 (78.4), Libya (78.2), Kenya (74.5), Tunisia (74.5), Uganda (72.9), while in JJA, Libya (92.1), Uganda (86.0), S. Sudan (82.2),  
Ethiopia (80.6) and Gabon (80.6) had the highest stringency index (Table S1). Interesting to notice that countries with lower  
stringency index which were below 50, such as Burundi, Niger, Tanzania, Zambia, and Somalia (Table S1), usually released  
their restriction earlier, meaning those countries usually have a higher stringency index in MAM than that in JJA (Fig. 1c).

120



**Figure 1: The stringency index weighted average in major African countries in MAM (a) and JJA (b), and the changes from MAM to JJA (c). Among them, the countries in white (Figure a, b) lack containment information.**

### 2.3 Surface air quality data

125 In this study, we used the long-term chemical reanalysis products constructed by NASA Jet Propulsion Laboratory  
 (<https://tes.jpl.nasa.gov/tes/chemical-reanalysis/products/two-hourly>, last accessed March 10, 2024). The chemical reanalysis  
 products used a multi-component satellite data assimilation system (Miyazaki et al., 2020c) to assimilate the results of CO,  
 NO<sub>2</sub>, SO<sub>2</sub>, O<sub>3</sub>, and HNO<sub>3</sub> measurements from multiple satellites. Data assimilation uses MICROC-CHASER predictive models  
 to simulate various processes, including transport, emissions, deposition, and chemical reactions such as ozone and aerosol  
 130 processes. Integrated Kalman filtering technique was employed to combine prior data (predictions) and observational data for  
 obtaining optimal state estimation (Miyazaki et al., 2020b). During the optimization of pollutant emission estimates, only total  
 combined emissions were optimized, while proportions of different emission categories from previous emission estimates were  
 applied at each grid point to obtain assimilated posterior anthropogenic emissions (Miyazaki et al., 2021). Prior surface NO<sub>x</sub>  
 and SO<sub>2</sub> emissions in 2020 were derived from the Hemispheric Transport of Air Pollution version 2.2 at a resolution of 0.1°  
 135 for the anthropogenic emission (Janssens-Maenhout et al., 2015), Global Fire Assimilation System version 1.2 at a resolution  
 of 0.1° for the fire emissions (Kaiser et al., 2012), and Global Emissions Initiative at a resolution of 0.5 degrees for the soil  
 NO<sub>x</sub> emission (Janssens-Maenhout et al., 2015; Kaiser et al., 2012; Yienger and Levy II, 1995). Lightning NO<sub>x</sub> sources in the  
 model were calculated using corresponding parameterizations at each model time step (Price and Rind, 1992). The emissions  
 in 2020 were constrained by various satellite measurements including NO<sub>2</sub>, SO<sub>2</sub>, CH<sub>4</sub>, CO, and ozone (O<sub>3</sub>), with the quality of  
 140 the reanalysis field evaluated using ozone detection as well as aircraft and satellite observations. Based on TROPOMI NO<sub>2</sub>  
 constraints at a resolution of 0.56°, ground-level NO<sub>x</sub> emissions in 2020 have been used to assess global tropospheric ozone  
 response to COVID-19 lockdown measures (Miyazaki et al., 2021).

## 2.4 Tropospheric column data for HCHO and NO<sub>2</sub>

To help explain the ozone changes in major African countries, we also obtained high-resolution monthly offline products of  
145 2020 HCHO and NO<sub>2</sub> vertical column densities (VCD) from the tropospheric emission monitoring internet service (TEMIS;  
<https://www.temis.nl/index.php>, last accessed March 20, 2024) (Van Geffen, 2017) for use from the TROPOspheric  
Monitoring Instrument (TROPOMI). We used bilinear interpolation to standardize the data resolution to 0.1°×0.1°. Subsequently, the African border shapefile was cut to obtain monthly and quarterly mean concentrations of HCHO and NO<sub>2</sub> across the grid of the main continent of Africa. Finally, we calculated the HCHO/NO<sub>2</sub> ratios for MAM and JJA in 2020.

## 150 2.5 Statistical analyses to quantify the air quality changes

For this study, we applied two distinct methods to quantify the air quality changes during the lockdown periods. Following  
previous studies (such as Chen et al. (2020a); Zhang et al. (2022); Li et al. (2023); Ma et al. (2024)), we first applied the  
quarterly dual anomalies method (also called the difference-to-differences method) by considering seasonal and long-term  
variations in air pollution. Specifically, for each country and grid cells in African, we calculated the air quality changes during  
155 the lockdown period compared with the pre-lockdown period (February) in 2020, and then compared these changes to those  
observed during the corresponding periods from reference years (2005-2019). We refer to these changes as quarterly dual  
anomalies. It can be understood as the rate changes at which the concentration of pollutants decreases or rises during the  
lockdown period compared with those during pre-lockdown.

Another method we referred as the quarterly anomalies, in which we calculated the seasonal concentrations differences  
160 between 2020 and the multi-year mean (from 2005 to 2019) for MAM and JJA individually. In addition, we also reported the  
rate of changes in pollutant concentration for each country, which was calculated by dividing the quarterly anomalies from the  
multi-year mean. By performing the Mann-Kendall trend analysis of seasonal changes for the major air pollutants from 2005  
to 2019 (Fig. S3), we found that the P-values were all greater than 0.05 in Africa, indicating that there was no significant air  
quality trends caused by either anthropogenic emissions or meteorological conditions in Africa. Thus, we assume the multi-  
165 year average from 2005 to 2019 will be representative of the hypothetical air quality in 2020 if no lockdown measures were  
implemented, and the quarterly anomalies we calculated were mainly attributed to the emission changes caused by the  
lockdown measures. To test this hypothesis, we also examined the air quality changes by calculating the differences between  
values in 2020 with 5-year average from 2015 to 2019 for both methods, and we found similar spatial patterns of air quality  
changes (Figs. S20-S26).

## 170 2.6 Random forest model prediction of pollutants

To isolate the influence of local meteorological changes, we have also applied a random forest (RF) model to predict the  
pollutants concentration in specific regions of Africa. We focus the countries in CA as there has been a significant decrease in  
CO levels in this region. We used the average daily values of each feature from February to August 2015-2019 as the training



set. The features included time (the day of the year), latitude and longitude, as well as meteorological variables such as  
175 temperature (T2), humidity, v wind, and u wind. The target variable was the CO concentration. All of the data are from the  
chemical reanalysis products constructed by NASA Jet Propulsion Laboratory ([https://tes.jpl.nasa.gov/tes/chemical-  
reanalysis/products/two-hourly](https://tes.jpl.nasa.gov/tes/chemical-reanalysis/products/two-hourly), last accessed March 10, 2024) and the resolution were uniformly adjusted to  $0.5^{\circ} \times 0.5^{\circ}$  using  
bilinear interpolation. These predictions are based on historical levels of CO, which include information on past anthropogenic  
emissions. Therefore, the predicted CO concentrations we obtain still retain the influence of emissions from previous years. In  
180 order to improve the accuracy, we simulated for February, MAM, and JJA separately. For model validation, we used a time  
series split rolling cross-verification based on five splits according to Shen et al. (2024), and the Pearson correlation coefficient  
(PCC) and low root mean square error (RMSE) were used to measure the performance of the model, as shown in Figure S12.  
After cross-validation, the optimal model was selected to predict the CO concentrations in 2020 under the previous emission  
scenario. The "n\_estimators" of the model was 108 and "max\_depth" was 21. Then, by subtracting the actual CO concentrations  
185 in 2020 from the predicted values, we can isolate the air quality changes from the meteorological conditions. Finally, calculate  
the average concentrations of CO for February, MAM, and JJA respectively.

## 2.7 Pearson correlation analyses

We then performed Pearson correlation analysis to examine the correlations between pollutants and stringency index or  
meteorological variables (Cahyono et al., 2023). We firstly calculated the average daily concentration anomalies for SO<sub>2</sub>, CO,  
190 NO<sub>2</sub>, temperature and absolute humidity from March 1 to August 31, 2020. The calculations of the average daily concentration  
anomalies were similar to the quarterly anomalies we described above. Then, the Pearson correlation coefficients of pollutant  
daily anomaly with temperature daily anomaly, absolute humidity daily anomaly and the stringency index were calculated  
from March 1 to May 31 and from June 1 to August 31, respectively.

## 3 Results

### 195 3.1 Changes in primary gas pollutants of CO, SO<sub>2</sub>, and NO<sub>2</sub>

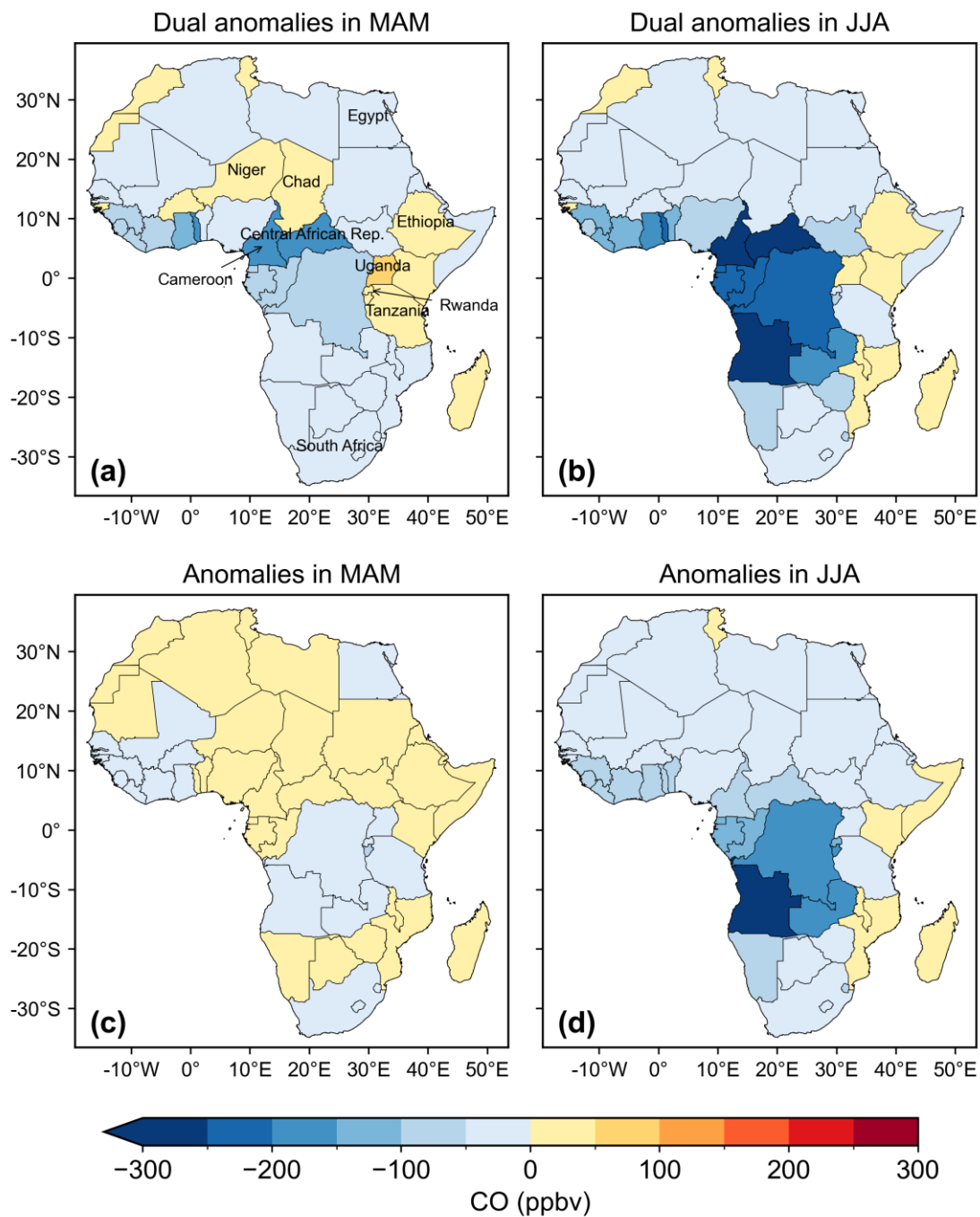
#### 3.1.1 CO changes

Figure 2 shows the spatial distribution of CO changes in MAM and JJA in African countries estimated from the two methods.  
In general, we found consistent temporal-spatial CO changes from the two methods, with larger CO decreases observed in JJA  
than those in MAM, sharing the similar spatial patterns with the country stringency index (Fig. 1). The average CO changes  
200 was -55 ppbv (-470 to 22 ppb depending on the country) in Africa during the JJA, compared with -0.10 ppb (-62 to 34 ppb) in  
MAM (Fig. 2c, d). Meanwhile, the two methods are consistent to show that the countries with the largest CO decline are  
mainly located in CA, such as Angola (Fig. 2b, d). Previous studies have shown that 90% of fires occurred in sub-Saharan  
regions were caused by human activities (Xiang et al., 2023; Shikwambana, 2019), especially in JJA the fire season in the



southern hemisphere (Fig. S4). Thus, we conclude that the constrained human activities during the strict lockdown periods in  
205 JJA (Fig. 1) reduced the occurrence of wildfires, and thus leading to the more significant CO decline. Further, light-duty  
vehicle was another major source of CO especially in the Sahara regions such as Egypt in NA (Mostafa et al., 2021), thus the  
stricter lockdown measures which restrained the vehicles activities contributed to reduce the CO concentration (Ukpebor et al.,  
2010). Besides the similar results we draw from the two methods, there are also slightly variations as well, with the quarterly  
210 dual anomalies method (Fig. 2a, b) usually showing larger CO decreases in both seasons. Also, we observed a hotspot for CO  
decreases in Cameroon and Central African Rep. in both seasons using the quarterly dual anomalies (Fig. 2a, b) which were  
missed by the quarterly anomalies method (Fig. 2c, d). We also found obvious CO increases in MAM especially in NA regions  
as estimated from the quarterly anomalies method (Fig. 2c), which could be caused by the high natural biomass burning activity  
in the northern hemisphere Africa (Hua et al., 2024) and less dense population (Fig. S29). To further investigate the  
215 contribution of emission changes on the concentration anomalies in 2020, we compared the CO concentration differences in  
MAM and JJA of 2020 between those estimated in the chemical reanalysis data with the RF-predicted CO concentration which  
isolated the influence of meteorological changes, and we found similar magnitude changes between these two, confirming our  
conclusions above (Fig. S11).





220 **Figure 2: Spatial distribution of CO changes from the two methods: quarterly dual anomalies (a, b), and quarterly anomalies (c, d) for MAM (a, c), JJA (b, d) in African countries. The units are ppbv.**

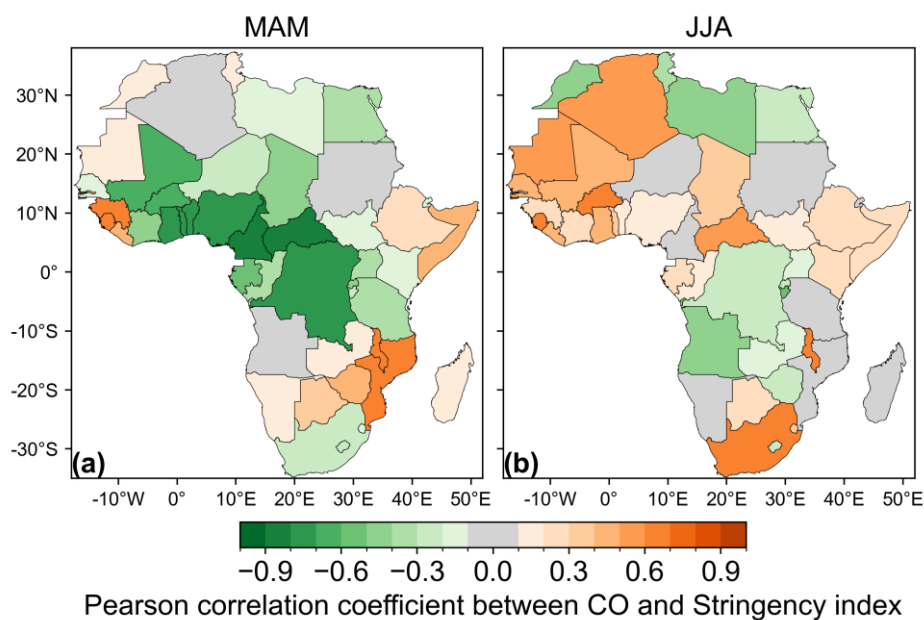


**Figure 3: Spatial distribution of pearson correlation coefficients from March 1<sup>st</sup> to May 31<sup>st</sup> (a), and June 1<sup>st</sup> to August 31<sup>st</sup> (b) in African countries. Positive values denote positive correlations and negative values denotes negative correlations between daily CO anomalies and stringency index.**

225

By calculating the Pearson correlation coefficient between CO anomalies and stringency index (Fig. 3), we found that during the MAM, many countries exhibited a significant negative correlation (Minimum is -0.86) between these two variables. This negative correlation was mainly concentrated in CA, WA and NA, such as Central African Republic, Cameroon, Nigeria, Egypt and South Africa. Although the Central African Republic had moderate lockdown stringency indexes and population levels, its CO concentration still significantly decreased due to its originally higher CO concentration, leading to more noticeable emission reductions. In contrast, despite lower original CO concentrations in Egypt and South Africa, their higher stringency indexes resulted in a decrease in CO concentrations. However, countries like Chad, Niger, Uganda, Rwanda, and Ethiopia still had positive dual anomalies, which may be related to lower stringency indexes in these countries or their neighbours, as well as lower CO concentrations (Fig. S4). During the JJA, the decrease in CO concentrations was negatively correlated with stringency indexes in only some countries, particularly in CA and NA. Because some countries have a lower level of stringency index during the JJA, the Pearson correlation analysis may be affected by unusual occasional changes in pollutants. In conclusion, changes in CO concentration are co-controlled by each country's individual CO emission levels, the lockdown stringency indexes and even population conditions.

240



### 3.1.2 NO<sub>2</sub> change

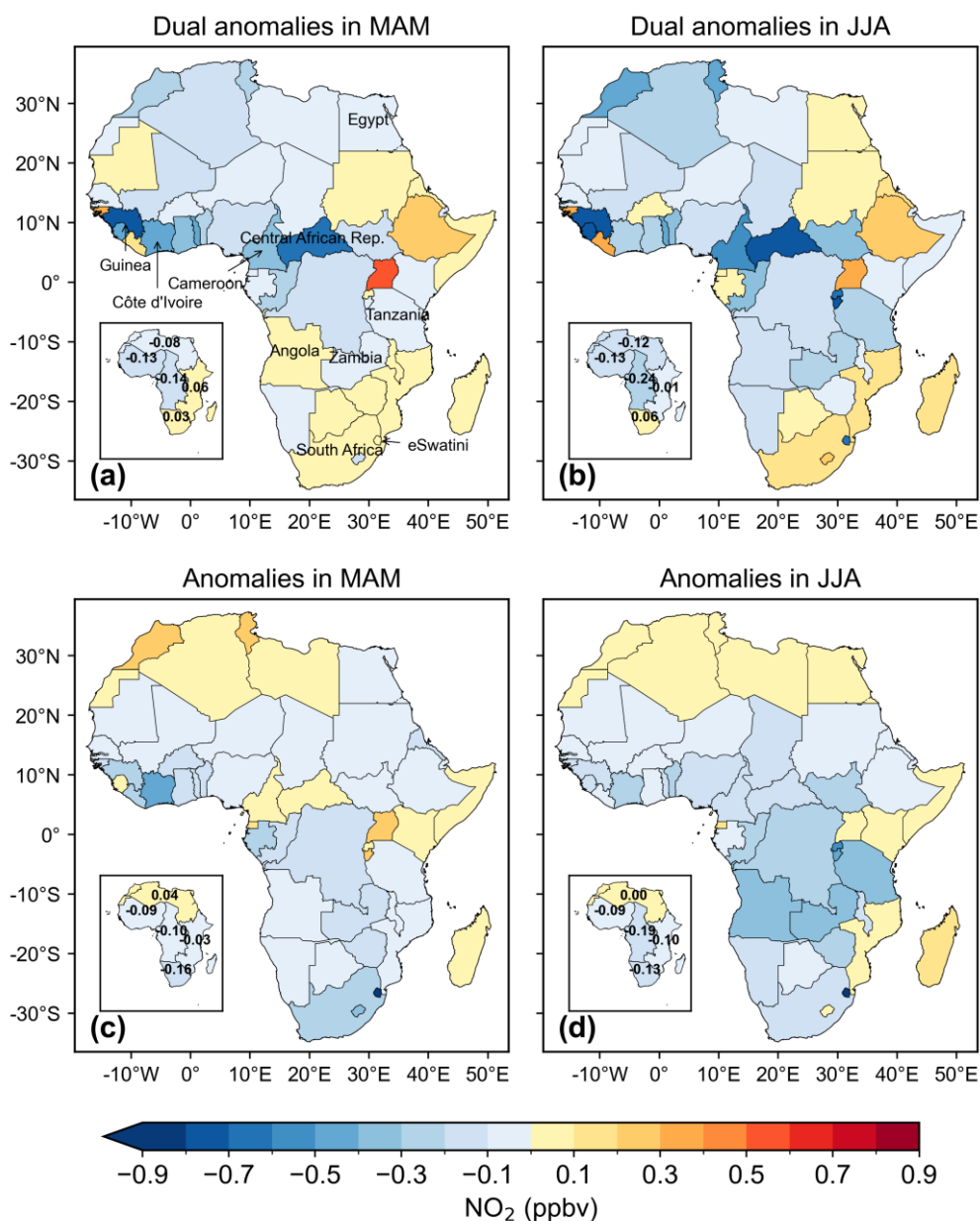


**Figure 4:** The same as Figure 2, but for NO<sub>2</sub>. The units are ppbv.

245 As shown in Fig. 4, the spatial NO<sub>2</sub> anomalies in MAM and JJA estimated from the two methods agree well with each other, similar as we observed for CO. We attribute the reduction in NO<sub>2</sub> concentration in CA and WA regions to reduced biomass burning and industrial emissions due to strict lockdown measures as also discussed in previous studies (Fawole et al., 2022;



250 Hickman et al., 2021). In most countries, the decreases in NO<sub>2</sub> during JJA were slightly larger than those during MAM, such as in the Central African Republic and Cameroon. This aligns with the overall trends in stringency index between the two seasons. In general, the average change in NO<sub>2</sub> across Africa during JJA is -0.09 ppb (-1.8 to 0.2 ppb, corresponding to a change rate of -29.9% to 30.1% depending on the country; see Fig. S31b), whereas during MAM, the average change is -0.05 ppb (-1.2 to 0.3 ppb, change rate between -38.8% and 23.4%). There are some countries that showed similar changes from both methods, such as Egypt, Chad, and Tanzania. In SA, the quarterly anomalies method showed an obvious decrease of NO<sub>2</sub> which were not captured by the quarterly dual anomalies method.

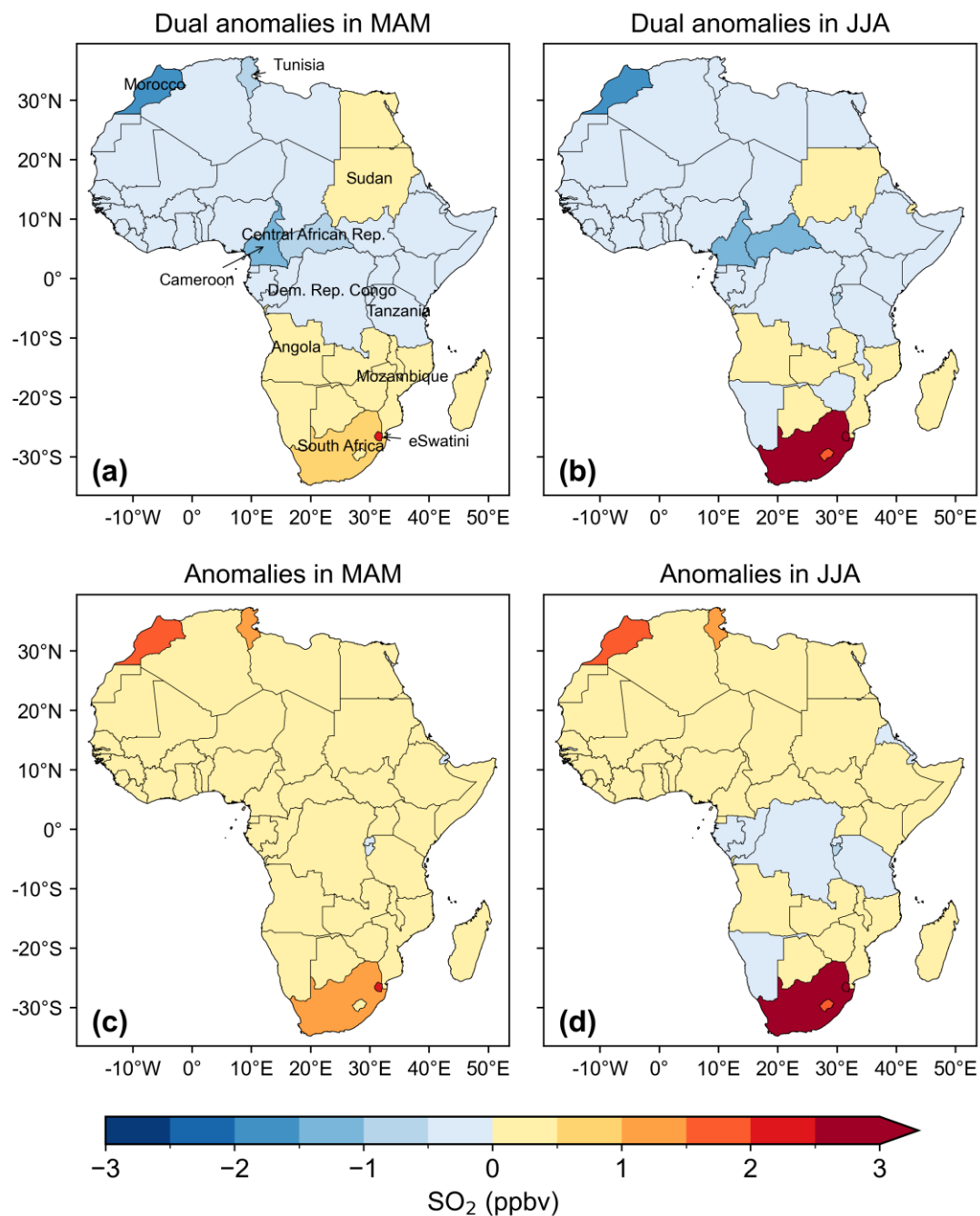
255

However, the countries showing the greatest declines differ between the two methods. The quarterly dual anomalies method shows the largest NO<sub>2</sub> decreases occur in WA and the northern parts of CA during MAM and JJA, such as in the Central African Republic (-0.6 and -0.8 ppbv), Cameroon (-0.3 and -0.5 ppbv), and Guinea (-0.8 and -0.7 ppbv). Conversely, quarterly anomalies method shows the greatest declines in NO<sub>2</sub> concentration in southern parts of CA and SA, such as eSwatini (-1.2 ppbv), South Africa (-0.3 ppbv), and Côte d'Ivoire (-0.4 ppbv) in MAM, and eSwatini (-1.8 ppbv) and Angola (-0.3 ppbv) in JJA. In addition, the quarterly dual anomalies showed NO<sub>2</sub> decreases in NA countries, such as Tunisia, Morocco, Algeria, and Libya, whereas the quarterly anomalies method showed an increase.

260



### 3.1.3 SO<sub>2</sub> change



265 **Figure 5:** The same as Figure 2, but for SO<sub>2</sub>.

Figure 5 illustrates the spatial distribution of SO<sub>2</sub> changes in MAM and JJA as estimated by two methods in African countries.



Surprisingly, there is substantial and even contradictory variation in SO<sub>2</sub> concentration changes between the two methods. The dual quarterly anomalies methods showed a general decrease in SO<sub>2</sub> (Fig. 5a, b), leading by Morocco (-1.62 ppbv), Cameroon (-1.45 ppbv), and the Central African Republic (-1.21 ppbv). However, the quarterly anomalies indicate widespread increases in SO<sub>2</sub> concentration in both seasons (Fig. 5c, d), with slightly noticeable decreases in countries like the Democratic Republic of Congo and Tanzania during JJA. We attributed this difference as the quarterly anomalies method indicates the rate changes at which the concentration of pollutants decreases or rises during the lockdown period compared with those during pre-lockdown, and we found higher SO<sub>2</sub> concentration in the WA and NA in Feb, 2020, which makes the relative comparisons with MAM and JJA in 2020 much lower. However, the anomalies method only considered the changes between the months in 2020 with corresponding months in years.

In addition, both methods indicated that in SA countries such as South Africa and Mozambique, the concentration of SO<sub>2</sub> continued to increase, which contradicts with the stringency index change. We attributed this increases to the possible expansion of coal-fired power plants in these countries (Dahiya et al., 2020; Agbo et al., 2021). On April 1st, 2020, this region doubled the emission limit for SO<sub>2</sub> from coal-fired power plants and allowed many factories to reopen after July 1<sup>st</sup> (Dahiya et al., 2020; Hale et al., 2021). Besides, the stay-at-home policy may actually increase residential electricity demand and residential fuel (Matandirotya et al., 2022; Adesina et al., 2022; Hersey et al., 2015), thereby increasing the operating load of power plants (Wetchayont and Levy, 2021) and then SO<sub>2</sub> concentrations. Meanwhile, the dry, cold conditions in the southern Hemisphere make it harder for SO<sub>2</sub> to disperse. Previous studies have observed that, apart from Africa, in some countries with high SO<sub>2</sub> emissions such as Turkey (Kotan and Erener, 2023) and India (Mor et al., 2021), certain cities also experienced an increase in SO<sub>2</sub> concentrations during lockdown periods (Mor et al., 2021; Mahato et al., 2020; Qayyum et al., 2023). This highlights the need for stricter coal restriction policies or promoting the use of clean energy to reduce environmental pollution in these regions. Therefore, containment policies implemented in winter may have a limited effect on SO<sub>2</sub> reduction in regions with heavy coal-burning industries and residential burnings.



290 **3.2 Ozone change**

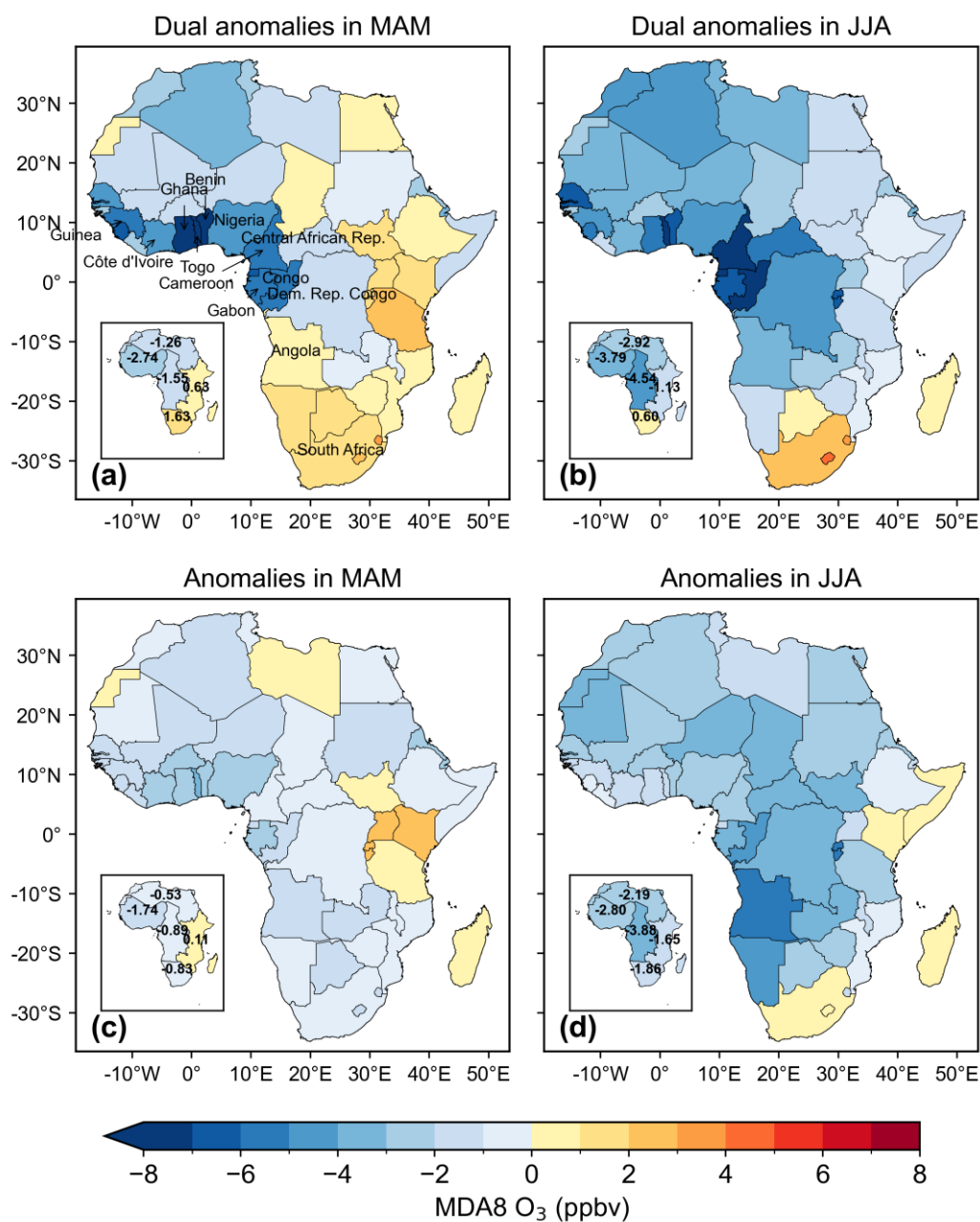


**Figure 6:** The same as Figure 2, but for MDA8 O<sub>3</sub>.

As shown in Fig. 6, both methods indicated a larger decline for the maximum daily 8-hour average (MDA8 O<sub>3</sub>) in African  
 295 during JJA than those during MAM. The JJA anomaly is -2.48 ppb (-5.98 to 0.35 ppb), ranging from -11.67% to 1.08%,

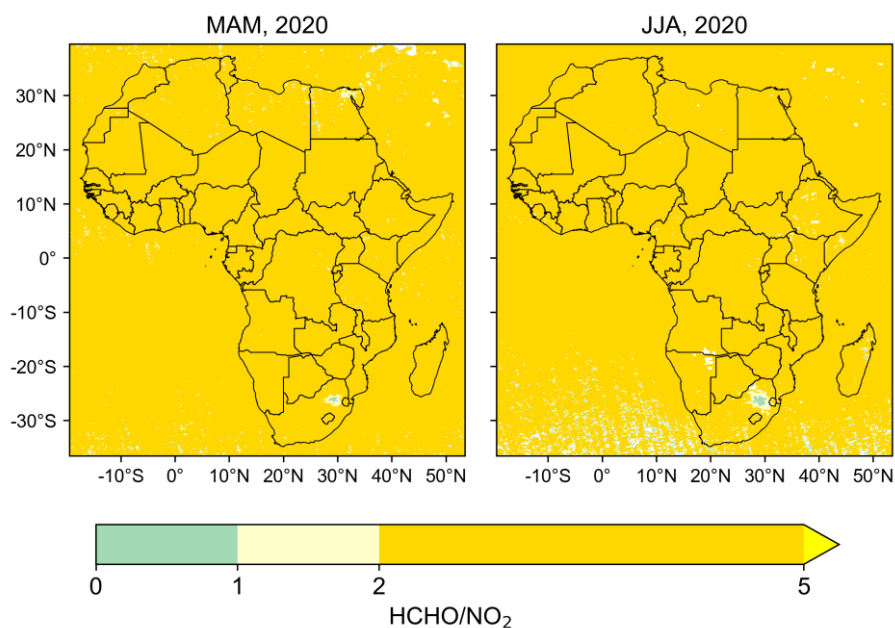


compared with an -0.74 ppb (-3.12 to 2.74 ppb, ranging from -10.99% to 7.54%) decreases in MAM (Fig. S32). Both methods agree with each other on the regions with the greatest declines. During MAM, the largest declines occur in the WA region, such as Togo (-9.37 from the dual anomaly method, and -3.12 ppbv for the anomaly method), Benin (-7.66 and -2.92 ppbv), and Ghana (-7.56 and -2.96 ppbv). In JJA (Fig. 6b, d), countries in the CA exhibit the most significant decreases, including  
300 Congo (-7.64 and -4.57 ppbv for dual anomaly and anomaly method respectively), Gabon (-6.03/-3.59 ppbv), and Central African Republic (-5.40/-3.47 ppbv). In regions with frequent biomass burning such as WA and CA, the decline in O<sub>3</sub> concentrations may be more closely related to reduced biomass burning emissions due to lockdown measures. We employed the ratio of satellite derived HCHO (representing VOCs) to NO<sub>2</sub> as an indicator to assess O<sub>3</sub> sensitivity to precursors in Africa (Nussbaumer et al., 2023; Choi et al., 2012; Duncan et al., 2010). We found that in many countries across WA, Central, and  
305 EA, such as Togo, Ghana, and Benin, anomalies in O<sub>3</sub> concentrations corresponded well with changes in NO<sub>2</sub> (Fig. 7). This alignment is attributed to higher levels of VOC/NO<sub>x</sub> ratios in regions abundant in tropical vegetation, where O<sub>3</sub> tends to correlate positively with NO<sub>x</sub>.

In South Africa, both methods showed a greater increase in O<sub>3</sub> concentrations during the JJA compared to MAM (Fig. 6),  
310 which may be associated with a decline in NO<sub>2</sub> concentrations. According to Fig. 7, during the JJA, industrial areas of South Africa exhibited broader ranges of lower HCHO/NO<sub>2</sub> ratio, indicating a negative correlation between O<sub>3</sub> and NO<sub>x</sub> (Laban et al., 2018). Significant reductions in NO<sub>x</sub> levels favors O<sub>3</sub> formation (Wang et al., 2019). Additionally, strong correlations between O<sub>3</sub> and CO in South Africa have been reported (Borduas-Dedekind et al., 2023), and Vakkari et al. (2020) documented rapid O<sub>3</sub> formation in plumes from grassland fires in South Africa, highlighting the substantial influence of biomass burning  
315 emissions on O<sub>3</sub> generation in SA. The O<sub>3</sub> increases during the lockdown were also seen in some regions of other countries, such as Shanghai (Tan and Wang, 2022), North China (Liu et al., 2021) and Milan in Italy (Zoran et al., 2020).

In both methods, a widespread decrease in surface O<sub>3</sub> across NA was observed, possibly influenced by ozone precursors and meteorological conditions, particularly temperature (Tang et al., 2021). Comparing with previous years, temperatures in the  
320 Sahara have notably decreased, particularly during JJA, with coastal regions experiencing a decline of 4°C (Fig. S27c). Lower temperatures might reduce the photolysis rate of ozone molecules, further stabilizing the atmosphere and making it less likely for O<sub>3</sub> to disperse, thereby leading to decreased surface O<sub>3</sub> concentrations.





325 **Figure 7: Spatial distribution of averaged HCHO/NO<sub>2</sub> ratios during MAM and JJA, 2020.**

### 3.3 Aerosol particles

The inorganic aerosols concentration changes, including sulfate, nitrate, ammonium aerosols, often exhibit nonlinear relationships due to their formation through both primary emissions and secondary reactions of gaseous precursors in the atmosphere (Gao et al., 2003). Etchie et al. (2021) found that meteorological conditions rather than lockdowns resulted in  
330 marginal reductions in aerosol levels in Nigeria. Similar observations of no significant reductions in atmospheric particulate matter due to lockdown measures have also been reported in China, United States, Spain, and India (Le et al., 2020; Li et al., 2021; Baldasano, 2020; Chen et al., 2020b; Vig et al., 2023).

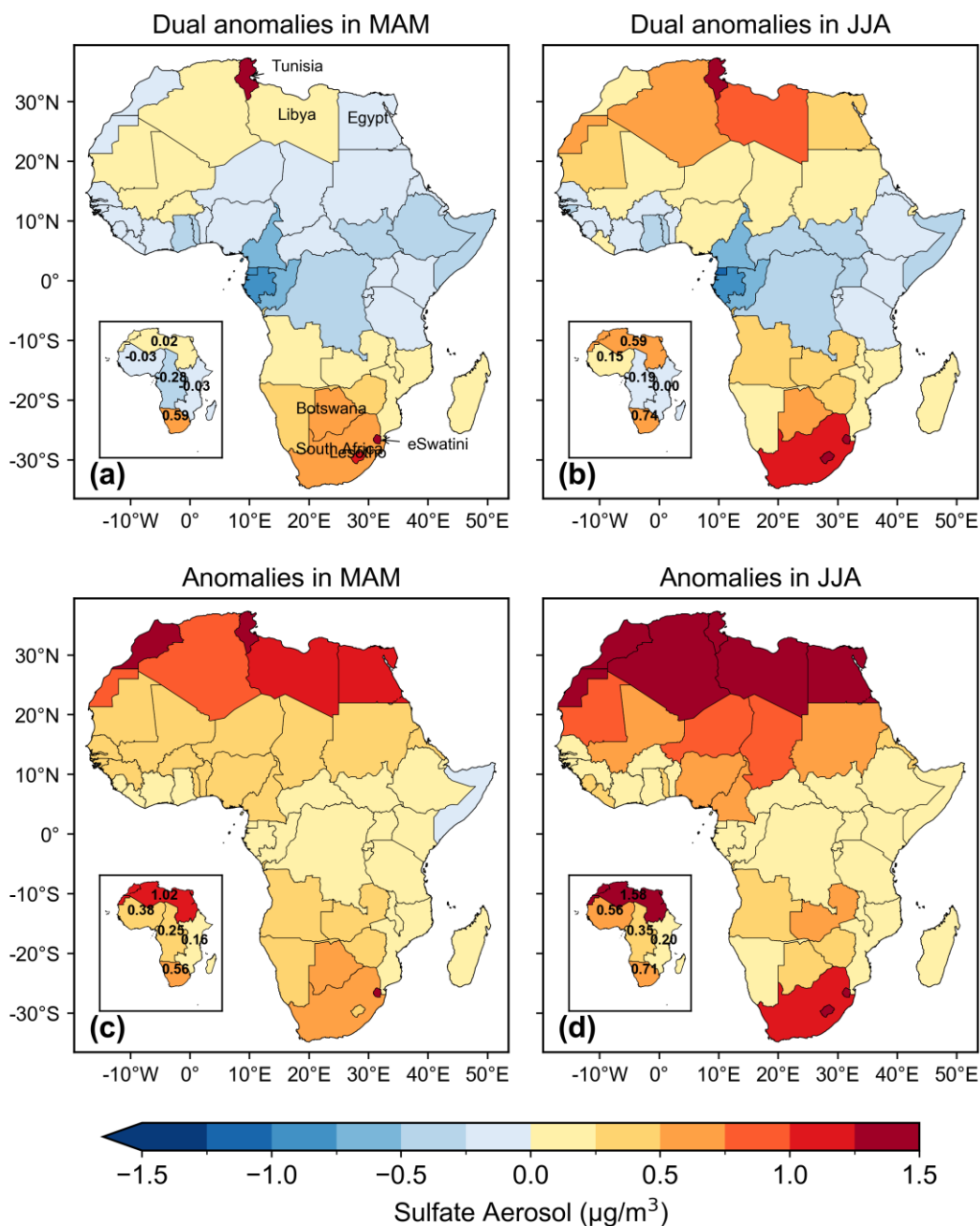


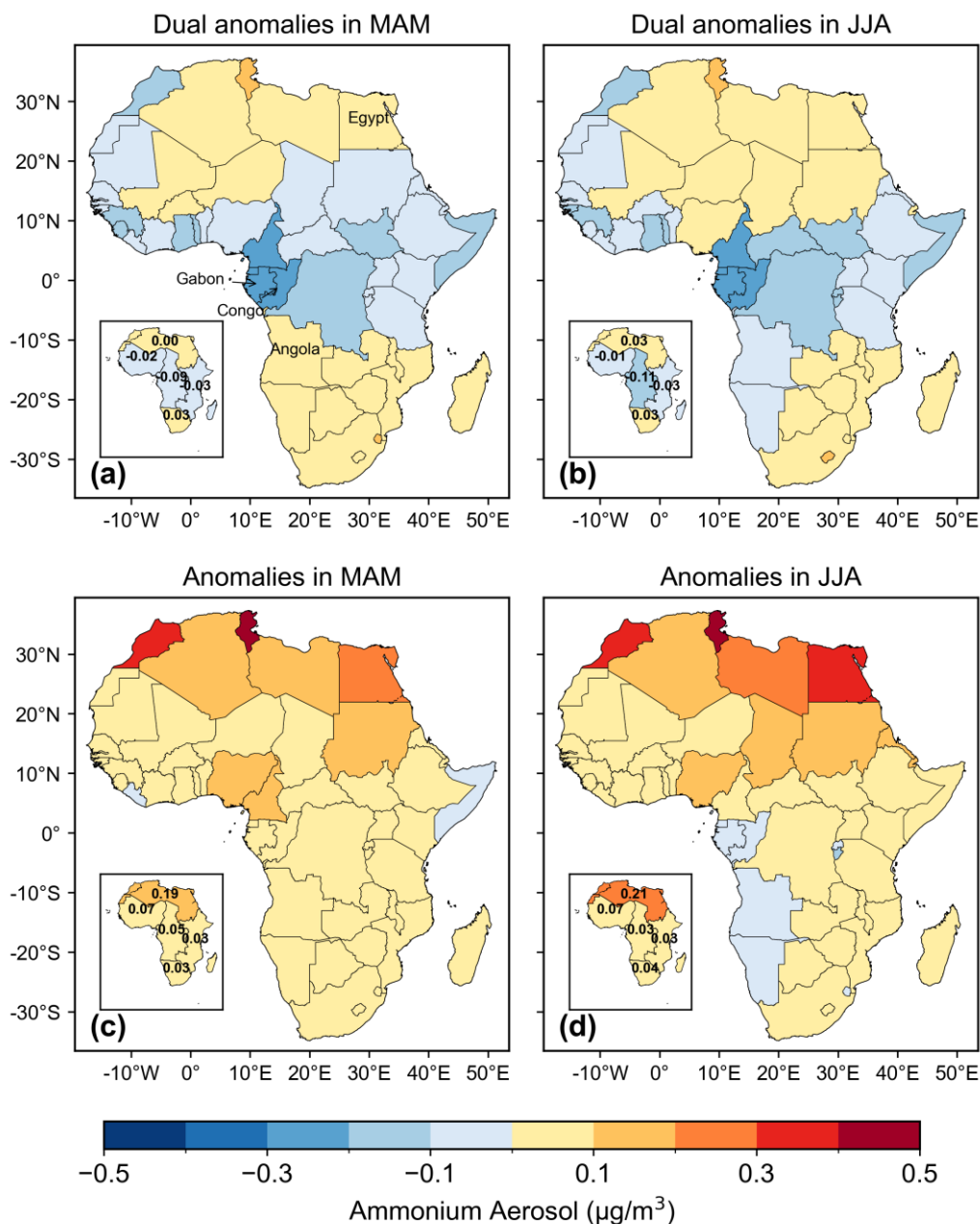
**Figure 8:** The same as Figure 2, but for sulfate aerosol.

335

Unlike other pollutants, both methods showed a greater increase for sulfate aerosols in JJA compared to MAM across Africa overall especially in NA and SA (Fig. 8). We estimated that the average sulphate aerosol particles in Africa were  $0.49 \mu\text{g}/\text{m}^3$  and  $0.72 \mu\text{g}/\text{m}^3$  for MAM and JJA respectively from the quarterly anomaly method (Fig.S34). NA, located in the Sahara Desert,



is the world's largest dust source (Huneeus et al., 2011). The increase in sulfate aerosol concentration was primarily influenced  
340 by Saharan dust pollution in June 2020 (Burgess and Oyola-Merced, 2024). Furthermore, the decrease in temperature during  
the JJA in NA regions compared to previous years also may favors the accumulation of aerosols (Lou et al., 2017; Singh et al.,  
2020a), thereby increasing aerosol particle concentrations. In SA, the significant increase in sulfate, particularly in South  
Africa, may be linked to increased coal combustion activities during lockdown periods. However, we also noticed that the two  
methods showed distinct results for sulfate aerosol changes in WA, CA, and EA regions, similar as we observed for the gaseous  
345 SO<sub>2</sub> (Fig. 5). The quarterly dual anomaly displayed an overall decrease in concentrations in these regions (Fig. 8a, b), whereas  
the quarterly anomaly shows a slight increase (Fig. 8c, d). This is linked to the elevated February concentrations of sulfate  
aerosols near the equator compared to previous years (Fig. S8d). The comprehensive analysis of both methods suggests that  
despite a relative increase in sulfate aerosol concentrations compared to previous years (Fig. S8 a,d), reduced fires due to  
pandemic lockdowns or meteorological conditions can mitigate the upward trend in sulfate concentrations. Similar to sulfate  
350 aerosol, we observed an increases of ammonium aerosol in both MAM and JJA in most countries (Fig. 9), especially in the  
NA and SA regions. We concluded that that ammonium existed mostly in the format of sulfate ammonium (Bhanarkar et al.,  
2005; Fattorini and Regoli, 2020), and was therefore influenced by biomass burning and soil emissions (e.g., animal manure,  
fertilizers) (Mor et al., 2021; Gordon et al., 2023).



355

**Figure 9:** The same as Figure 2, but for ammonium aerosol.

As shown in Fig. 10, unlike sulfate and ammonium aerosols, the nitrate aerosol showed consistent decreases from the two methods in major African countries. For instance, using the quarterly anomalies method, the average MAM anomaly in Africa is  $-0.01 \mu\text{g}/\text{m}^3$ , ranging from  $-0.23$  to  $0.06 \mu\text{g}/\text{m}^3$  ( $-89.45\%$  to  $114.27\%$ , Fig. S36), while the JJA anomaly is  $-0.04 \mu\text{g}/\text{m}^3$ ,

360



365 ranging from  $-0.64$  to  $0.004 \mu\text{g}/\text{m}^3$  ( $-74.50\%$  to  $47.22\%$ ). Both methods showed a greater decrease in JJA compared to MAM  
across Africa, particularly in countries such as Angola, Zambia, and eSwatini. Relative to other aerosol particles, nitrate aerosol  
particles primarily depend on emissions of nitrogen oxides from human activities in the atmosphere, such as traffic, industrial  
activities, and construction (Agbo et al., 2021). Therefore, during the pandemic, restrict traffic measures from lockdown lead  
370 to more pronounced reductions in nitrogen dioxide levels, thereby affecting nitrate aerosol production. In regions with higher  
nitrate, such as Egypt, Tunisia, and Angola (Fig. S9), the magnitude of concentration decrease was also greater, consistent  
with previous findings (Mostafa et al., 2021). We observed that in some countries with lower stringency index of lockdown  
measures (such as below 60), including Niger, Burkina Faso and Ethiopia, pollutant concentrations decreased slowly or even  
increased. This suggests that in Africa, the wide-ranging decrease in nitrate aerosol concentrations due to lockdown measures  
may not have been uniformly observed.

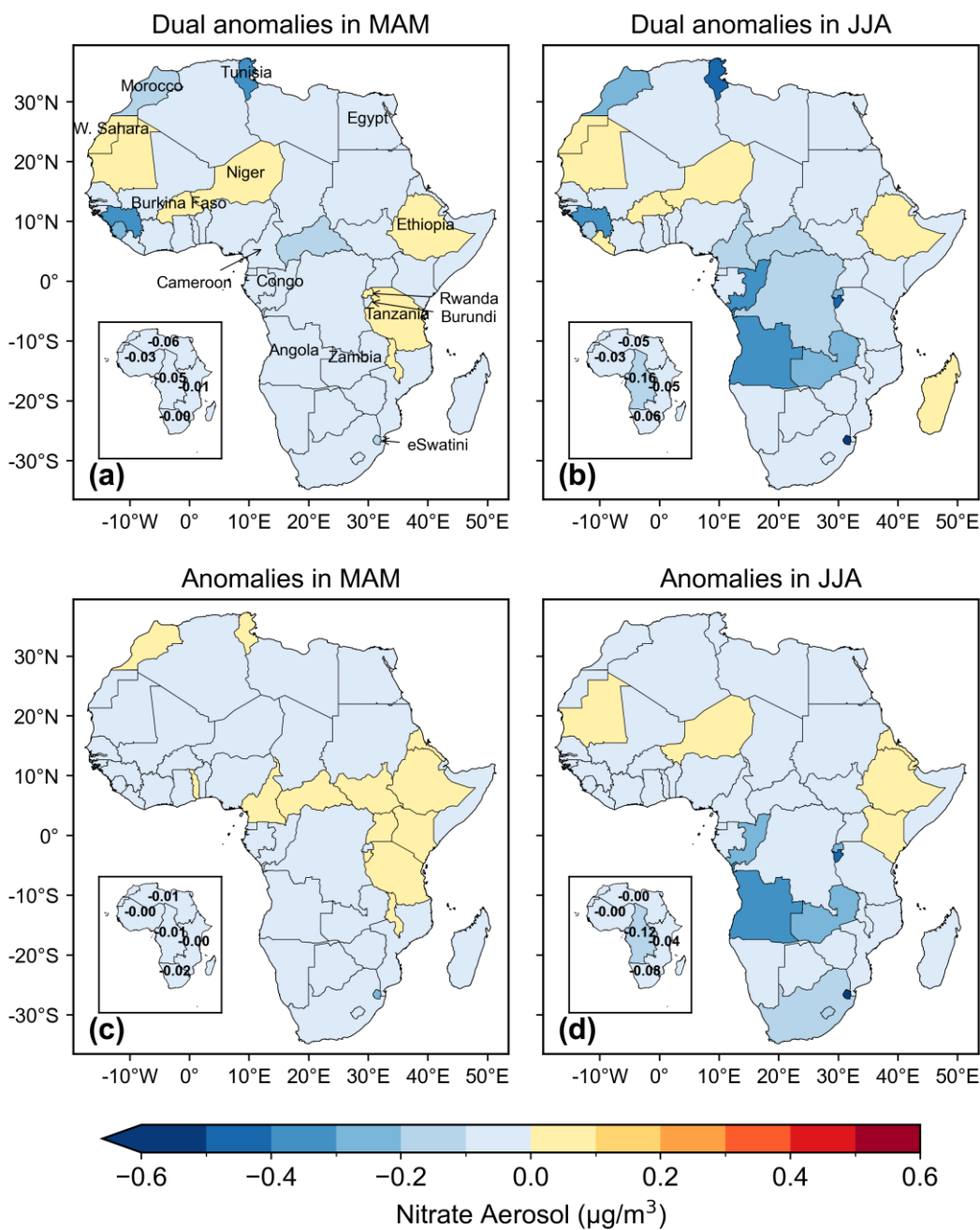


Figure 10: The same as Figure 2, but for nitrate aerosol.



#### 375 **4 Summary and conclusions**

This study analyzed the impact of lockdown policies on the changes of gaseous pollutants in African countries, focusing on CO, NO<sub>2</sub>, SO<sub>2</sub>, O<sub>3</sub>, and aerosols particles. We applied two distinct methods, quarterly dual anomalies and quarterly anomalies to calculate the concentration changes in MAM (March to May) and JJA (June to August) in 2020. The quarterly dual anomalies calculated the air quality changes during the lockdown period compared with the pre-lockdown period (February),  
380 and then compared these changes to corresponding periods from reference years (2005 - 2019). The quarterly anomalies calculated the seasonal concentrations differences between 2020 and the multi-year mean (2005 - 2019) for MAM and JJA individually.

1. Both methods revealed decrease in CO concentrations in majority African countries, with greater reductions observed during JJA compared to MAM. We attributed this to the emissions reductions from biomass burning (sub-Saharan) and the transport emissions (Saharan) which was both caused by the restricted human activities during the lockdown (Hua et al., 2024; Mostafa et al., 2021). The random forest model further corroborated the significant role of anthropogenic emission changes in the observed reduction of CO concentrations in CA.  
385
2. Both methods observed a decrease in NO<sub>2</sub> concentrations across most African countries, with a slightly larger reduction in JJA compared to MAM, demonstrating the effectiveness of restrictions on traffic, biomass burning, and industrial activity. However, discrepancies were observed in the NA region, where the quarterly dual anomalies method indicated a decline in NO<sub>2</sub>, while the quarterly anomalies method showed an increase. This suggests that while NO<sub>2</sub> levels were generally higher in February 2020 compared to previous years, the containment measures, especially traffic restrictions (Mostafa et al., 2021) mitigated the rate of increase.  
390
3. Unexpectedly, both methods observed an increase in SO<sub>2</sub> in South Africa, especially during JJA. This increase may be linked to relaxed emission limits for factory pollutants and heightened coal-fired power plant usage during home isolation in winter (Dahiya et al., 2020; Hale et al., 2021). For most other countries, the quarterly dual anomalies method revealed a general decline in SO<sub>2</sub>, whereas the quarterly anomalies indicated an increase. This shows that despite an overall increase in SO<sub>2</sub> levels in 2020, containment measures may have slowed the rate of increase.  
395
4. Regarding MDA8 O<sub>3</sub>, both methods indicated a general decline in concentrations in most countries, especially in WA and CA regions, with greater reductions observed during JJA. This decline is likely related to reduced emissions from biomass combustion as a result of lockdown measures. However, in South Africa, a more significant increase in O<sub>3</sub> during JJA was noted, potentially due to decreased NO<sub>2</sub> concentrations and lower tropospheric HCHO/NO<sub>2</sub> ratios.  
400
5. Both methods revealed an increase in sulfate and ammonium aerosols in the NA and SA regions, with a larger increase during JJA. In the NA region, this increase is likely associated with an extreme dust event in June 2020, while in the SA region, it corresponds to increased coal burning (Simelane and Langerman, 2023). Nitrate aerosols consistently decreased across both quarters, reflecting the overall reduction in NO<sub>2</sub> emissions due to containment measures.  
405

In conclusion, the air quality changes during lockdown in Africa may be interweaving with both natural and anthropogenic influences. Judging the similarities and disagreements from the two methods applied in this study, we highlight the necessity to include more surface observations for African countries, as well as stricter emission standards for coal-fired plants and promote clean energy infrastructures.

**Acknowledgements:** We acknowledge the use of data products from the TROPES Project (TROpospheric Ozone and its Precursors from Earth System Sounding) which is a NASA funded activity under the NASA Earth Science Mission Directorate (SMD) program called Ozone Trends Science (OTS).

**Author contributions:** YZ and ZH designed the study; KZ and ZH acquired the data, ZH performed data analysis, prepared the plots and tables, wrote the paper with the help from ZL, ZW, BL. All authors conducted research and wrote and edited this manuscript.

**Competing interests:** The authors declare that they have no competing interests.

**Data and materials availability:** All the data required to assess the conclusions in the paper are present within the paper and/or supplementary materials. The baseline concentration and emission data used in the study can be freely downloaded from NASA Goddard Earth Sciences Data and Information Services Center (GES DISC) (<https://disc.gsfc.nasa.gov/information/data-release?title=Release%20of%20TROPES%20Chemical%20Reanalysis%20Products>, last accessed September 10<sup>th</sup>, 2024).

## Appendix A. Supporting Information

Supplementary figures and tables associated with this article can be found in the online version at...

## References

- Abisha Meji, M., Milon, S. D., and M, M.: Effect of Covid-19 Induced Lockdown on Air Quality in Kampala, *i-manager's Journal on Future Engineering and Technology*, 16, <https://doi.org/10.26634/jfet.16.1.17546>, 2020.
- Adesina, J. A., Piketh, S. J., Burger, R. P., and Mkhathshwa, G.: Assessment of criteria pollutants contributions from coal-fired plants and domestic solid fuel combustion at the South African industrial highveld, *Cleaner Engineering and Technology*, 6, 100358, <https://doi.org/10.1016/j.clet.2021.100358>, 2022.
- Agbo, K. E., Walgraeve, C., Eze, J. I., Ugwoke, P. E., Ukoha, P. O., and Van Langenhove, H.: A review on ambient and indoor air pollution status in Africa, *Atmos. Pollut. Res.*, 12, 243-260, <https://doi.org/10.1016/j.apr.2020.11.006>, 2021.
- Baldasano, J. M.: COVID-19 lockdown effects on air quality by NO<sub>2</sub> in the cities of Barcelona and Madrid (Spain), *Sci. Total Environ.*, 741, 140353, <https://doi.org/10.1016/j.scitotenv.2020.140353>, 2020.
- Bhanarkar, A. D., Goyal, S. K., Sivacoumar, R., and Chalapati Rao, C. V.: Assessment of contribution of SO<sub>2</sub> and NO<sub>2</sub> from different sources in Jamshedpur region, India, *Atmos. Environ.*, 39, 7745-7760, <https://doi.org/10.1016/j.atmosenv.2005.07.070>, 2005.
- Borduas-Dedekind, N., Naidoo, M., Zhu, B., Geddes, J., and Garland, R. M.: Tropospheric ozone (O<sub>3</sub>) pollution in Johannesburg, South Africa: Exceedances, diurnal cycles, seasonality, O<sub>x</sub> chemistry and O<sub>3</sub> production rates, *Clean Air J.*, 33, <https://doi.org/10.17159/caj/2023/33/1.15367>, 2023.





- Burgess, R. W. and Oyola-Merced, M. I.: Radiative Examination of Developing African Easterly Waves and Saharan Dust Interactions: Comparative Insights from Reanalysis and NASA Airborne Observations, *EGUsphere*, 2024, 1-26, <https://doi.org/10.5194/egusphere-2023-2972>, 2024.
- 445 Cahyono, W. E., Anwar, A., Gusnita, D., Rahmatia, F., Santoso, H., Kombara, P. Y., Sumaryati, Setyawati, W., Sari, W. J., Susilowati, Y., Kartika, T., Putra, A. Y., and Romadona, N. F.: Assessment of Air Quality Before and After the COVID-19 Pandemic in Indonesia, in: *Urban Commons, Future Smart Cities and Sustainability*, edited by: Chatterjee, U., Bandyopadhyay, N., Setiawati, M. D., and Sarkar, S., Springer International Publishing, Cham, 957-979, [https://doi.org/10.1007/978-3-031-24767-5\\_41](https://doi.org/10.1007/978-3-031-24767-5_41), 2023.
- 450 Chen, K., Wang, M., Huang, C., Kinney, P. L., and Anastas, P. T.: Air pollution reduction and mortality benefit during the COVID-19 outbreak in China, *Lancet Planet.*, 4, e210-e212, [https://doi.org/10.1016/s2542-5196\(20\)30107-8](https://doi.org/10.1016/s2542-5196(20)30107-8), 2020a.
- Chen, L. A., Chien, L. C., Li, Y., and Lin, G.: Nonuniform impacts of COVID-19 lockdown on air quality over the United States, *Sci. Total Environ.*, 745, 141105, <https://doi.org/10.1016/j.scitotenv.2020.141105>, 2020b.
- 455 Chen, L. W. A., Chien, L.-C., Li, Y., and Lin, G.: Nonuniform impacts of COVID-19 lockdown on air quality over the United States, *Sci. Total Environ.*, 745, 141105, <https://doi.org/10.1016/j.scitotenv.2020.141105>, 2020c.
- Choi, Y., Kim, H., Tong, D., and Lee, P.: Summertime weekly cycles of observed and modeled NO<sub>x</sub> and O<sub>3</sub> concentrations as a function of satellite-derived ozone production sensitivity and land use types over the Continental United States, *Atmos. Chem. Phys.*, 12, 6291-6307, <https://doi.org/10.5194/acp-12-6291-2012>, 2012.
- 460 Chossière, G. P., Xu, H., Dixit, Y., Isaacs, S., Eastham, S. D., Allroggen, F., Speth, R. L., and Barrett, S. R. H.: Air pollution impacts of COVID-19–related containment measures, *Sci. Adv.*, 7, <https://doi.org/10.1126/sciadv.abe1178>, 2021.
- Collivignarelli, M. C., Abbà, A., Bertanza, G., Pedrazzani, R., Ricciardi, P., and Carnevale Miino, M.: Lockdown for CoViD-2019 in Milan: What are the effects on air quality?, *Sci. Total Environ.*, 732, 139280, <https://doi.org/10.1016/j.scitotenv.2020.139280>, 2020.
- 465 Dahiya, S., Anhäuser, A., Farrow, A., Thieriot, H., Chanchal, A., and Myllyvirta, L.: Ranking the World's Sulfur Dioxide (SO<sub>2</sub>) Hotspots: 2019-2020, Delhi: Center for Research on Energy and Clean Air & Greenpeace India, 4 pp [https://www.greenpeace.to/greenpeace/wp-content/uploads/2020/11/2020-so2report\\_lowres.pdf](https://www.greenpeace.to/greenpeace/wp-content/uploads/2020/11/2020-so2report_lowres.pdf), 2020.
- Duncan, B. N., Yoshida, Y., Olson, J. R., Sillman, S., Martin, R. V., Lamsal, L., Hu, Y., Pickering, K. E., Retscher, C., Allen, D. J., and Crawford, J. H.: Application of OMI observations to a space-based indicator of NO<sub>x</sub> and VOC controls on surface ozone formation, *Atmos. Environ.*, 44, 2213-2223, <https://doi.org/10.1016/j.atmosenv.2010.03.010>, 2010.
- 470 Etchie, T. O., Etchie, A. T., Jauro, A., Pinker, R. T., and Swaminathan, N.: Season, not lockdown, improved air quality during COVID-19 State of Emergency in Nigeria, *Sci. Total Environ.*, 768, 145187, <https://doi.org/10.1016/j.scitotenv.2021.145187>, 2021.
- Fattorini, D. and Regoli, F.: Role of the chronic air pollution levels in the Covid-19 outbreak risk in Italy, *Environ. Pollut.*, 264, 114732, <https://doi.org/10.1016/j.envpol.2020.114732>, 2020.
- 475 Fawole, O. G., Yusuf, N., Sunmonu, L. A., Obafaye, A., Audu, D. K., Onuorah, L., Olusegun, C. F., Deme, A., and Senghor, H.: Impacts of COVID-19 Restrictions on Regional and Local Air Quality Across Selected West African Cities, *GeoHealth*, 6, e2022GH000597, <https://doi.org/10.1029/2022GH000597>, 2022.
- Fisher, S., Bellinger, D. C., Cropper, M. L., Kumar, P., Binagwaho, A., Koudenoukpo, J. B., Park, Y., Taghian, G., and Landrigan, P.: Air pollution and development in Africa: impacts on health, the economy, and human capital, *Lancet Planet.*, 5, e681-e688, [https://doi.org/10.1016/S2542-5196\(21\)00201-1](https://doi.org/10.1016/S2542-5196(21)00201-1), 2021.
- 480 Fuwape, I. A., Okpalaonwuka, C. T., and Ogunjo, S. T.: Impact of COVID -19 pandemic lockdown on distribution of inorganic pollutants in selected cities of Nigeria, *Air Qual. Atmos. Hlth.*, 14, 149-155, <http://doi.org/10.1007/s11869-020-00921-8>, 2020.
- Gao, S., Hegg, D. A., Hobbs, P. V., Kirchstetter, T. W., Magi, B. I., and Sadilek, M.: Water-soluble organic components in aerosols associated with savanna fires in southern Africa: Identification, evolution, and distribution, *J. Geophys. Res.-Atmos.*, 108, <https://doi.org/10.1029/2002JD002324>, 2003.
- 485 Garcia, L., Johnson, R., Johnson, A., Abbas, A., Goel, R., Tatah, L., Damsere-Derry, J., Kyere-Gyeabour, E., Tainio, M., de Sá, T. H., and Woodcock, J.: Health impacts of changes in travel patterns in Greater Accra Metropolitan Area, Ghana, *Environ. Int.*, 155, 106680, <https://doi.org/10.1016/j.envint.2021.106680>, 2021.
- 490 Goldberg, D. L., Anenberg, S. C., Griffin, D., McLinden, C. A., Lu, Z., and Streets, D. G.: Disentangling the Impact of the COVID-19 Lockdowns on Urban NO<sub>2</sub> From Natural Variability, *Geophys. Res. Lett.*, 47, e2020GL089269, <https://doi.org/10.1029/2020GL089269>, 2020.



- Gordon, J. N. D., Bilsback, K. R., Fiddler, M. N., Pokhrel, R. P., Fischer, E. V., Pierce, J. R., and Bililign, S.: The Effects of Trash, Residential Biofuel, and Open Biomass Burning Emissions on Local and Transported PM<sub>2.5</sub> and Its Attributed Mortality in Africa, *GeoHealth*, 7, <https://doi.org/10.1029/2022GH000673>, 2023.
- 495 Hale, T., Angrist, N., Goldszmidt, R., Kira, B., Petherick, A., Phillips, T., Webster, S., Cameron-Blake, E., Hallas, L., Majumdar, S., and Tatlow, H.: A global panel database of pandemic policies (Oxford COVID-19 Government Response Tracker), *Nat. Hum. Behav.*, 5, 529-538, <https://doi.org/10.1038/s41562-021-01079-8>, 2021.
- Health Effects Institute: The State of Air Quality and Health Impacts in Africa. A Report from the State of Global Air Initiative, Boston, MA:Health Effects Institute, <https://www.stateofglobalair.org/sites/default/files/documents/2022-10/the-state-of-air-quality-and-health-impacts-in-africa-press-release.pdf>, 2022.
- 500 Hersey, S. P., Garland, R. M., Crosbie, E., Shingler, T., Sorooshian, A., Piketh, S., and Burger, R.: An overview of regional and local characteristics of aerosols in South Africa using satellite, ground, and modeling data, *Atmos. Chem. Phys.*, 15, 4259-4278, 10.5194/acp-15-4259-2015, 2015.
- Hickman, J. E., Andela, N., Tsigaridis, K., Galy-Lacaux, C., Ossohou, M., Dammers, E., Van Damme, M., Clarisse, L., and Bauer, S. E.: Continental and Ecoregion-Specific Drivers of Atmospheric NO<sub>2</sub> and NH<sub>3</sub> Seasonality Over Africa Revealed by Satellite Observations, *Global Biogeochemical Cycles*, 35, e2020GB006916, <https://doi.org/10.1029/2020GB006916>, 2021.
- 505 Hua, W., Lou, S., Huang, X., Xue, L., Ding, K., Wang, Z., and Ding, A.: Diagnosing uncertainties in global biomass burning emission inventories and their impact on modeled air pollutants, *Atmos. Chem. Phys.*, 24, 6787-6807, <https://doi.org/10.5194/acp-24-6787-2024>, 2024.
- 510 Huneus, N., Schulz, M., Balkanski, Y., Griesfeller, J., Prospero, J., Kinne, S., Bauer, S., Boucher, O., Chin, M., Dentener, F., Diehl, T., Easter, R., Fillmore, D., Ghan, S., Ginoux, P., Grini, A., Horowitz, L., Koch, D., Krol, M. C., Landing, W., Liu, X., Mahowald, N., Miller, R., Morcrette, J. J., Myhre, G., Penner, J., Perlwitz, J., Stier, P., Takemura, T., and Zender, C. S.: Global dust model intercomparison in AeroCom phase I, *Atmos. Chem. Phys.*, 11, 7781-7816, <https://doi.org/10.5194/acp-11-7781-2011>, 2011.
- 515 Janssens-Maenhout, G., Crippa, M., Guizzardi, D., Dentener, F., Muntean, M., Pouliot, G., Keating, T., Zhang, Q., Kurokawa, J., Wankmüller, R., Denier van der Gon, H., Kuenen, J. J. P., Klimont, Z., Frost, G., Darras, S., Koffi, B., and Li, M.: HTAP\_v2.2: a mosaic of regional and global emission grid maps for 2008 and 2010 to study hemispheric transport of air pollution, *Atmos. Chem. Phys.*, 15, 11411-11432, <https://doi.org/10.5194/acp-15-11411-2015>, 2015.
- Kaiser, J. W., Heil, A., Andreae, M. O., Benedetti, A., Chubarova, N., Jones, L., Morcrette, J. J., Razinger, M., Schultz, M. G., Suttie, M., and van der Werf, G. R.: Biomass burning emissions estimated with a global fire assimilation system based on observed fire radiative power, *Biogeosciences*, 9, 527-554, <https://doi.org/10.5194/bg-9-527-2012>, 2012.
- 520 Katoto, P. D. M. C., Byamungu, L., Brand, A. S., Mokaya, J., Strijdom, H., Goswami, N., De Boever, P., Nawrot, T. S., and Nemery, B.: Ambient air pollution and health in Sub-Saharan Africa: Current evidence, perspectives and a call to action, *Environ. Res.*, 173, 174-188, <https://doi.org/10.1016/j.envres.2019.03.029>, 2019.
- 525 Kganyago, M. and Shikwambana, L.: Did COVID-19 Lockdown Restrictions have an Impact on Biomass Burning Emissions in Sub-Saharan Africa?, *Aerosol Air. Qual. Res.*, 21, 200470, <https://doi.org/10.4209/aaqr.2020.07.0470> 2021.
- Khomsi, K., Najmi, H., Amghar, H., Chelhaoui, Y., and Souhaili, Z.: COVID-19 national lockdown in morocco: Impacts on air quality and public health, *One Health*, 11, <https://doi.org/10.1016/j.onehlt.2020.100200>, 2020.
- 530 Khomsi, K., Najmi, H., Amghar, H., Chelhaoui, Y., and Souhaili, Z.: COVID-19 national lockdown in morocco: Impacts on air quality and public health, *One Health*, 11, 100200, <https://doi.org/10.1016/j.onehlt.2020.100200>, 2021.
- Kotan, B. and Erener, A.: Seasonal analysis and mapping of air pollution (PM<sub>10</sub> and SO<sub>2</sub>) during Covid-19 lockdown in Kocaeli (Turkiye), *International Journal of Engineering and Geosciences*, 8, 173-187, <https://doi.org/10.26833/ijeg.1111699>, 2023.
- Laban, T. L., van Zyl, P. G., Beukes, J. P., Vakkari, V., Jaars, K., Borduas-Dedekind, N., Josipovic, M., Thompson, A. M., Kulmala, M., and Laakso, L.: Seasonal influences on surface ozone variability in continental South Africa and implications for air quality, *Atmos. Chem. Phys.*, 18, 15491-15514, <https://doi.org/10.5194/acp-18-15491-2018>, 2018.
- 535 Le, T., Wang, Y., Liu, L., Yang, J., Yung, Y. L., Li, G., and Seinfeld, J. H.: Unexpected air pollution with marked emission reductions during the COVID-19 outbreak in China, *Science*, 369, 702-706, <https://doi.org/10.1126/science.abb7431>, 2020.
- Li, H., Zheng, B., Ciais, P., Boersma, K. F., Riess, T. C. V. W., Martin, R. V., Broquet, G., van der A, R., Li, H., Hong, C., Lei, Y., Kong, Y., Zhang, Q., and He, K.: Satellite reveals a steep decline in China's CO<sub>2</sub> emissions in early 2022, *Sci. Adv.*, 9, eadg7429, <https://doi.org/10.1126/sciadv.adg7429>, 2023.
- 540



- Li, M., Wang, T., Xie, M., Li, S., Zhuang, B., Fu, Q., Zhao, M., Wu, H., Liu, J., Saikawa, E., and Liao, K.: Drivers for the poor air quality conditions in North China Plain during the COVID-19 outbreak, *Atmos. Environ.*, 246, 118103, <https://doi.org/10.1016/j.atmosenv.2020.118103>, 2021.
- 545 Liu, Y., Wang, T., Stavrakou, T., Elguindi, N., Doumbia, T., Granier, C., Bouarar, I., Gaubert, B., and Brasseur, G. P.: Diverse response of surface ozone to COVID-19 lockdown in China, *Sci. Total Environ.*, 789, 147739, <https://doi.org/10.1016/j.scitotenv.2021.147739>, 2021.
- Lou, C., Liu, H., Li, Y., Peng, Y., Wang, J., and Dai, L.: Relationships of relative humidity with PM<sub>2.5</sub> and PM<sub>10</sub> in the Yangtze River Delta, China, *Environ. Monit. Assess.*, 189, <https://doi.org/10.1007/s10661-017-6281-z>, 2017.
- 550 Ma, Y., Nobile, F., Marb, A., Dubrow, R., Kinney, P. L., Peters, A., Stafoggia, M., Breitner, S., and Chen, K.: Air pollution changes due to COVID-19 lockdowns and attributable mortality changes in four countries, *Environ. Int.*, 187, 108668, <https://doi.org/10.1016/j.envint.2024.108668>, 2024.
- Mahato, S., Pal, S., and Ghosh, K. G.: Effect of lockdown amid COVID-19 pandemic on air quality of the megacity Delhi, India, *Sci. Total Environ.*, 730, 139086, <https://doi.org/10.1016/j.scitotenv.2020.139086>, 2020.
- 555 Matandirotya, N. R., Moletsane, S. D., Matandirotya, E., and Burger, R. P.: State of ambient air quality in a low-income urban settlement of South Africa, *Sci. Afr.*, 16, e01201, <https://doi.org/10.1016/j.sciaf.2022.e01201>, 2022.
- Mead, M. I., Okello, G., Mbandi, A. M., and Pope, F. D.: Spotlight on air pollution in Africa, *Nat. Geosci.*, 16, 930-931, <https://doi.org/10.1038/s41561-023-01311-2>, 2023.
- Miyazaki, K., Bowman, K. W., Yumimoto, K., Walker, T., and Sudo, K.: Evaluation of a multi-model, multi-constituent assimilation framework for tropospheric chemical reanalysis, *Atmos. Chem. Phys.*, 20, 931-967, <https://doi.org/10.5194/acp-20-931-2020>, 2020a.
- 560 Miyazaki, K., Bowman, K., Sekiya, T., Takigawa, M., Neu, J. L., Sudo, K., Osterman, G., and Eskes, H.: Global tropospheric ozone responses to reduced NO<sub>x</sub> emissions linked to the COVID-19 worldwide lockdowns, *Sci. Adv.*, 7, eabf7460, <https://doi.org/10.1126/sciadv.abf7460>, 2021.
- 565 Miyazaki, K., Bowman, K., Sekiya, T., Jiang, Z., Chen, X., Eskes, H., Ru, M., Zhang, Y., and Shindell, D.: Air Quality Response in China Linked to the 2019 Novel Coronavirus (COVID-19) Lockdown, *Geophys. Res. Lett.*, 47, e2020GL089252, <https://doi.org/10.1029/2020GL089252>, 2020b.
- Miyazaki, K., Bowman, K., Sekiya, T., Eskes, H., Boersma, F., Worden, H., Livesey, N., Payne, V. H., Sudo, K., Kanaya, Y., Takigawa, M., and Ogochi, K.: Updated tropospheric chemistry reanalysis and emission estimates, TCR-2, for 2005–2018, *Earth Syst. Sci. Data*, 12, 2223-2259, <https://doi.org/10.5194/essd-12-2223-2020>, 2020c.
- 570 Mor, S., Kumar, S., Singh, T., Dogra, S., Pandey, V., and Ravindra, K.: Impact of COVID-19 lockdown on air quality in Chandigarh, India: Understanding the emission sources during controlled anthropogenic activities, *Chemosphere*, 263, 127978, <https://doi.org/10.1016/j.chemosphere.2020.127978>, 2021.
- Mostafa, M. K., Gamal, G., and Wafiq, A.: The impact of COVID 19 on air pollution levels and other environmental indicators - A case study of Egypt, *J. Environ. Manage.*, 277, <https://doi.org/10.1016/j.jenvman.2020.111496>, 2021.
- 575 Muhammad, S., Long, X., and Salman, M.: COVID-19 pandemic and environmental pollution: A blessing in disguise?, *Sci. Total Environ.*, 728, 138820, <https://doi.org/10.1016/j.scitotenv.2020.138820>, 2020.
- Navaratnam, A. M. D., Williams, H., Sharp, S. J., Woodcock, J., and Khreis, H.: Systematic review and meta-analysis on the impact of COVID-19 related restrictions on air quality in low- and middle-income countries, *Sci. Total Environ.*, 908, <https://doi.org/10.1016/j.scitotenv.2023.168110>, 2024.
- 580 Navinya, C., Patidar, G., and Phuleria, H. C.: Examining Effects of the COVID-19 National Lockdown on Ambient Air Quality across Urban India, *Aerosol Air. Qual. Res.*, 20, 1759-1771, <https://doi.org/10.4209/aaqr.2020.05.0256> 2020.
- Nussbaumer, C. M., Fischer, H., Lelieveld, J., and Pozzer, A.: What controls ozone sensitivity in the upper tropical troposphere?, *Atmos. Chem. Phys.*, 23, 12651-12669, <https://doi.org/10.5194/acp-23-12651-2023>, 2023.
- 585 Pepe, E., Bajardi, P., Gauvin, L., Privitera, F., Lake, B., Cattuto, C., and Tizzoni, M.: COVID-19 outbreak response: a first assessment of mobility changes in Italy following national lockdown, medRxiv, <https://doi.org/10.1101/2020.03.22.20039933>, 2020.
- Price, C. and Rind, D.: A simple lightning parameterization for calculating global lightning distributions, *J. Geophys. Res.-Atmos.*, 97, 9919-9933, <https://doi.org/10.1029/92JD00719>, 1992.



- 590 Qayyum, F., Tariq, S., Nawaz, H., ul-Haq, Z., Mehmood, U., and Babar, Z. B.: Variation of air pollutants during COVID-19  
lockdown phases in the mega-city of Lahore (Pakistan); Insights into meteorological parameters and atmospheric chemistry,  
*Acta Geophys.*, <https://doi.org/10.1007/s11600-023-01208-z>, 2023.
- Qu, Z., Jacob, D. J., Silvern, R. F., Shah, V., Campbell, P. C., Valin, L. C., and Murray, L. T.: US COVID-19 Shutdown  
Demonstrates Importance of Background NO<sub>2</sub> in Inferring NO<sub>x</sub> Emissions From Satellite NO<sub>2</sub> Observations, *Geophys. Res.  
Lett.*, 48, e2021GL092783, <https://doi.org/10.1029/2021GL092783>, 2021.
- 595 Sekiya, T., Miyazaki, K., Eskes, H., Bowman, K., Sudo, K., Kanaya, Y., and Takigawa, M.: The worldwide COVID-19  
lockdown impacts on global secondary inorganic aerosols and radiative budget, *Sci. Adv.*, 9, eadh2688,  
<https://doi.org/10.1126/sciadv.adh2688>, 2023.
- Shen, F., Hegglin, M. I., and Yuan, Y.: Impact of weather patterns and meteorological factors on PM<sub>2.5</sub> and O<sub>3</sub> responses to  
the COVID-19 lockdown in China, *Atmos. Chem. Phys.*, 24, 6539-6553, <https://doi.org/10.5194/acp-24-6539-2024>, 2024.
- 600 Shi, Z., Song, C., Liu, B., Lu, G., Xu, J., Van Vu, T., Elliott, R. J. R., Li, W., Bloss, W. J., and Harrison, R. M.: Abrupt but  
smaller than expected changes in surface air quality attributable to COVID-19 lockdowns, *Sci. Adv.*, 7, eabd6696,  
<https://doi.org/10.1126/sciadv.abd6696>, 2021.
- Shikwambana, L.: Long-term observation of global black carbon, organic carbon and smoke using CALIPSO and MERRA-2  
data, *Remote Sens. Lett.*, 10, 373-380, <https://doi.org/10.1080/2150704X.2018.1557789>, 2019.
- 605 Siciliano, B., Carvalho, G., da Silva, C. M., and Arbilla, G.: The Impact of COVID-19 Partial Lockdown on Primary Pollutant  
Concentrations in the Atmosphere of Rio de Janeiro and São Paulo Megacities (Brazil), *B. Environ. Contam. Tox.*, 105, 2-8,  
<https://doi.org/10.1007/s00128-020-02907-9>, 2020.
- Sikarwar, A. and Rani, R.: Assessing the Immediate Effect of Covid-19 Lockdown on Air Quality: A Case Study of Delhi,  
India, *Journal of Environmental Geography*, 13, 27-33, <https://doi.org/10.2478/jengeo-2020-0009>, 2020.
- 610 Simelane, S. P. and Langerman, K. E.: The sensitivity of health impact assessments of PM<sub>2.5</sub> from South African coal-fired  
power stations, *Air Qual. Atmos. Hlth.*, <https://doi.org/10.1007/s11869-023-01447-5>, 2023.
- Singh, R. P. and Chauhan, A.: Impact of lockdown on air quality in India during COVID-19 pandemic, *Air Qual. Atmos. Hlth.*,  
13, 921-928, <https://doi.org/10.1007/s11869-020-00863-1>, 2020.
- 615 Singh, V., Biswal, A., Kesarkar, A. P., Mor, S., and Ravindra, K.: High resolution vehicular PM<sub>10</sub> emissions over megacity  
Delhi: Relative contributions of exhaust and non-exhaust sources, *Sci. Total Environ.*, 699, 134273,  
<https://doi.org/10.1016/j.scitotenv.2019.134273>, 2020a.
- Singh, V., Singh, S., Biswal, A., Kesarkar, A. P., Mor, S., and Ravindra, K.: Diurnal and temporal changes in air pollution  
during COVID-19 strict lockdown over different regions of India, *Environ. Pollut.*, 266, 115368,  
<https://doi.org/10.1016/j.envpol.2020.115368>, 2020b.
- 620 Tan, Y. and Wang, T.: What caused ozone pollution during the 2022 Shanghai lockdown? Insights from ground and satellite  
observations, *Atmos. Chem. Phys.*, 22, 14455-14466, <https://doi.org/10.5194/egusphere-2022-738>, 2022.
- Tang, R., Huang, X., Zhou, D., Wang, H., Xu, J., and Ding, A.: Global air quality change during the COVID-19 pandemic:  
Regionally different ozone pollution responses COVID-19, *Atmos. Ocean. Sci. Lett.*, 14,  
<https://doi.org/10.1016/j.aosl.2020.100015>, 2021.
- 625 Ukpebor, E. E., Ukpebor, J. E., Eromomene, F., Odiase, J. I., and Okoro, D.: Spatial and diurnal variations of Carbon monoxide  
(CO) pollution from motor vehicles in an Urban centre, *Pol. J. Environ. Stud.*, 19, 817-823, [https://www.pjoes.com/Spatial-  
and-Diurnal-Variations-of-Carbon-Monoxide-CO-Pollution-from-Motor-Vehicles,88452,0,2.html](https://www.pjoes.com/Spatial-and-Diurnal-Variations-of-Carbon-Monoxide-CO-Pollution-from-Motor-Vehicles,88452,0,2.html), 2010.
- Vakkari, V., Beukes, J. P., Josipovic, M., and van Zyl, P. G.: Observations of ozone formation in southern African savanna  
and grassland fire plumes, *Atmos. Environ.*, 223, 117256, <https://doi.org/10.1016/j.atmosenv.2019.117256>, 2020.
- 630 van Geffen, J. H. G. M., Eskes, H.J., Boersma, K.F., Maasackers, J.D. and Veeffkind, J.P.: TROPOMI ATBD of the total and  
tropospheric NO<sub>2</sub> data products, <https://api.semanticscholar.org/CorpusID:13794419>,
- Varga, G., Csávic, A., Szeberényi, J., and Gresina, F.: Non-uniform tropospheric NO<sub>2</sub> level changes in European Union  
caused by governmental COVID-19 restrictions and geography, *City and Environment Interactions*, 22,  
<https://doi.org/10.1016/j.cacint.2024.100145>, 2024.
- 635 Venter, Z. S., Aunan, K., Chowdhury, S., and Lelieveld, J.: COVID-19 lockdowns cause global air pollution declines, *Proc.  
Natl. Acad. Sci.*, 117, 18984-18990, <https://doi.org/10.1073/pnas.2006853117>, 2020.



- Vig, N., Ravindra, K., and Mor, S.: Environmental impacts of Indian coal thermal power plants and associated human health risk to the nearby residential communities: A potential review, *Chemosphere*, 341, <https://doi.org/10.1016/j.chemosphere.2023.140103>, 2023.
- 640 Wang, N., Lyu, X., Deng, X., Huang, X., Jiang, F., and Ding, A.: Aggravating O<sub>3</sub> pollution due to NO<sub>x</sub> emission control in eastern China, *Sci. Total Environ.*, 677, 732-744, <https://doi.org/10.1016/j.scitotenv.2019.04.388>, 2019.
- Wang, P., Chen, K., Zhu, S., Wang, P., and Zhang, H.: Severe air pollution events not avoided by reduced anthropogenic activities during COVID-19 outbreak, *Resour. Conserv. Recycl.*, 158, 104814, <https://doi.org/10.1016/j.resconrec.2020.104814>, 2020.
- 645 Wetchayont, P. and Levy, I.: Investigation on the Impacts of COVID-19 Lockdown and Influencing Factors on Air Quality in Greater Bangkok, Thailand, *Adv. Meteorol.*, 2021, 1-11, <https://doi.org/10.1155/2021/6697707>, 2021.
- Xiang, M., Xiao, C., Feng, Z., and Ma, Q.: Global distribution, trends and types of active fire occurrences, *Sci. Total Environ.*, 902, 166456, <https://doi.org/10.1016/j.scitotenv.2023.166456>, 2023.
- Yienger, J. J. and Levy II, H.: Empirical model of global soil-biogenic NO<sub>x</sub> emissions, *J. Geophys. Res.-Atmos.*, 100, 11447-11464, <https://doi.org/10.1029/95JD00370>, 1995.
- 650 Yusuf, N., Said S, R., Tilmes, S., and Gbobaniyi, E.: Multi-year analysis of aerosol optical properties at various timescales using AERONET data in tropical West Africa, *J. Aerosol Sci.*, 151, 105625, <https://doi.org/10.1016/j.jaerosci.2020.105625>, 2021.
- Zhang, J., Cui, K., Wang, Y.-F., Wu, J.-L., Huang, W.-S., Wan, S., and Xu, K.: Temporal Variations in the Air Quality Index and the Impact of the COVID-19 Event on Air Quality in Western China, *Aerosol Air. Qual. Res.*, 20, 1552-1568, <http://doi.org/10.4209/aaqr.2020.06.0297>, 2020.
- Zhang, Y., Zhao, B., Jiang, Y., Xing, J., Sahu, S. K., Zheng, H., Ding, D., Cao, S., Han, L., Yan, C., Duan, X., Hu, J., Wang, S., and Hao, J.: Non-negligible contributions to human health from increased household air pollution exposure during the COVID-19 lockdown in China, *Environ. Int.*, 158, 106918, <https://doi.org/10.1016/j.envint.2021.106918>, 2022.
- 660 Zoran, M. A., Savastru, R. S., Savastru, D. M., and Tautan, M. N.: Assessing the relationship between ground levels of ozone (O<sub>3</sub>) and nitrogen dioxide (NO<sub>2</sub>) with coronavirus (COVID-19) in Milan, Italy, *Sci. Total Environ.*, 740, 140005, <https://doi.org/10.1016/j.scitotenv.2020.140005>, 2020.